A Molecular Synchrotron

Cynthia E. Heiner[1], David Carty[1§], Gerard Meijer[1], and Hendrick L. Bethlem[1,2]

[1]*Fritz-Haber-Institut der Max-Planck-Gesellschaft, Faradayweg 4-6, Berlin, Germany*
[2]*Laser Centre Vrije Universiteit, De Boelelaan 1081, NL-1081HV, Amsterdam, The Netherlands*

Many of the tools for manipulating the motion of neutral atoms and molecules take their inspiration from techniques developed for charged particles. Traps for atoms – akin to the Paul trap for ions[1] - have paved the way for many exciting experiments, ranging from ultra precise clocks[2] to creating quantum degenerate matter[3,4]. Surprisingly, little attention has been paid to developing a neutral particle analog of a synchrotron – arguably, the most celebrated tool of the charged particle physicist[5,6]. To date, the few experiments dealing with ring structures for neutral particles have employed cylindrically symmetric designs[7-9]; in these rings, no force is applied to the particles along the longitudinal direction and the stored particles are free to fill the entire ring. We demonstrate here a synchrotron for neutral polar molecules. A packet of ammonia molecules is accelerated, decelerated and focused along the longitudinal direction ("bunched") using the fringe fields between the two halves of a segmented hexapole ring. The stored bunch of cold molecules (T=0.5 mK) is confined to a 3 mm packet even after a flight distance of over 30 meters (40 roundtrips). Furthermore, we show the injection of multiple packets into the ring.

In traps, electromagnetic fields are used to keep particles confined in a region of space where they can be studied in complete isolation from the (hot) environment. In its simplest form, a

§ Present address: Physical and Theoretical Chemistry Laboratory, South Parks Road, Oxford OX1 3QZ, United Kingdom

storage ring is a trap in which the particles – rather than having a minimum potential energy at a single location in space – have a minimum potential energy on a circle. Storage rings like these have been demonstrated for neutrons[7], atoms[8], and molecules[9]. The advantage of a storage ring over a trap is that packets of particles with a non-zero mean velocity can be confined. While circling the ring, these particles can be made to interact repeatedly, at well defined times and at distinct positions with electromagnetic fields and/or other particles. To fully exploit the possibilities offered by a ring structure, it is imperative that the particles remain in a bunch as they revolve around the ring. This ensures a high density of stored particles, moreover, this makes it possible to inject multiple – either co-linear or counter propagating – packets into the ring without affecting the packet(s) already stored.

In order to provide the necessary force(s) to bunch the molecules, the cylindrical symmetry of the ring must be broken; as a consequence, the transverse confining force will vary as a function of the longitudinal position in the ring. The variation of the confinement force has major consequences for the stability of the particles's trajectories. For certain longitudinal velocities, the disturbance caused by the longitudinal focusing elements ('bunchers') will add up, meaning that all trajectories become unstable and those particles will be lost. These unstable velocity regions are known as 'stop bands' in charged particle accelerator physics[5,6]. To minimize the width of these bands, corrective elements ('correcters') need to be implemented. Here, we demonstrate a molecular synchrotron based on a simple scheme to incorporate these necessary elements proposed by Crompvoets et al.[10]. A more elaborate design for a synchrotron was published by Nishimura et al.[11]. In a different approach, Murch et al.[12] observed a reduced dispersion of ultracold atoms propagating at velocities close to a stop band in an atomic storage ring.

Our synchrotron, depicted in Fig. 1, consists of two hexapoles bent into a semi-circle separated by a 2 mm gap. By switching the voltages applied to the electrodes, as shown in Figure 1(a)-(d), the necessary fields are created for confinement, to perform stop band correction, for

acceleration/deceleration and bunching, and to extract laser-ionized molecules, respectively. In the lower part of Figure 1 a time sequence is shown for a round trip. In normal operation, the voltages are applied (as in Fig. 1(a)) such that the resulting electric field is zero at the center and increases linearly radially outwards. Molecules in states that have a positive energy shift in the applied electric field – so-called low-field seekers – will experience a force towards the center of the hexapole. In a curved hexapole, the molecules also experience a centrifugal force that depends on their forward velocity. At a certain radius, the inward force due to the Stark potential and the outward centrifugal force will cancel. For example, a ND_3 molecule in the $|J,K\rangle = |1,1\rangle$ low-field-seeking state flying with a forward velocity of 87 m/s will be displaced radially outwards by 2 mm from the geometric center of the hexapole. As this hypothetical molecule revolves around the ring, it will form a closed orbit that remains at this radial position. Molecules flying with the same forward velocity but with a different radial position or with a non-zero radial velocity will oscillate around this closed orbit with a frequency of around 600 Hz.

In the gap region, the molecules can be both accelerated/decelerated and bunched by applying the voltages shown in Fig. 1(c) to one bend, while the other bend is kept at a ground potential. As molecules enter the gap, they are exposed to a field gradient that causes the molecules to gain Stark energy and consequently lose kinetic energy, i.e. the molecules are decelerated. As the molecules exit the gap, however, they are exposed to an opposing field gradient that causes the molecules to lose Stark energy and thus gain kinetic energy, i.e. the molecules are accelerated. The time sequence is synchronized to the position (and velocity) of one hypothetical molecule, appropriately referred to as the `synchronous` molecule – assuring that this molecule is always at the same position in the gap when the fields are switched. It will, therefore, lose or gain the same amount of kinetic energy per round trip. It follows that molecules in front of the synchronous molecule will lose more kinetic energy as the synchronous molecule. Vice versa, molecules that are behind the synchronous molecule will gain more kinetic energy as the synchronous molecule. As a result, the molecules within a small position and velocity interval will experience a force towards the

synchronous molecule and will oscillate around it; the molecules are trapped in a traveling potential well that revolves around the ring. This concept is known as phase stability[13,14] and forms the basis of all modern charged particle accelerators and storage rings. An extensive discussion of the application of phase stability for decelerating polar molecules in so-called Stark decelerators can be found elsewhere[15,16].

In the gap the molecules are not transversely confined. We compensate for this by increasing the focusing force during a short period of time before and after the molecules pass through the gap, by switching to the correcter configuration shown in Fig 1(b). For detection, the stored molecules are ionized and extracted perpendicularly to the plane of the ring, using the configuration shown in Fig 1 (d), and then counted by an ion detector.

In our experiments, the synchrotron is injected with packets of Stark-decelerated ammonia molecules. Both the mean value and the width of the velocity distribution of the injected beam is tunable; details of the injection beam line can be found elsewhere[17]. Fig. 2 shows the ammonia density in the detection zone of the ring as a function of storage time. The velocity of the stored packet is kept at 87 m/s, implying that the molecules take about 9.3 ms to make one round trip in the 81 cm circumference ring. After an initial rapid decrease, and some modulations, the signal is seen to become relatively constant. Starting from about the 20^{th} round trip, the signal decays with a 1/e time of 0.5 seconds, consistent with losses due to collisions with background gas in our 2×10^{-8} mbar vacuum.

The time-of-flight (TOF) profile for each round trip shown in Fig. 2 was fitted to a Gaussian. From these fits we infer the position spread of the stored packet in the detection region, plotted as circles in Fig. 3(a). The width of the packet is seen to decrease until after about the 20^{th} round trip, after which it stabilizes around a value of 3 mm. To determine the longitudinal temperature of the packet in the ring, we have measured the expansion rate of the packet in the absence of the buncher. The inset of Fig. 3(a) shows the expansions when the molecules are

released from the longitudinal well after the 4^{th} and 25^{th} round trip, indicated by triangles (△) and squares (□), respectively. The solid lines in the inset show the results from a simple formula fitted to the expansions. We find the velocity spread of the packet released after the 4^{th} round trip to be 1.7 m/s, corresponding to 1.3 mK, and after the 25^{th} round trip to be 1.1 m/s, corresponding to 0.5 mK. Although initially confined, the hottest molecules are slowly expelled due to coupling between the longitudinal and transverse motions, causing the initial decrease in the position spread and temperature. As both the width and the temperature of the packet stay constant for the later round trips, we conclude that the trajectories of these molecules are stable and they will, in principle, be confined indefinitely.

From the Gaussians fitted to the data shown in Fig. 2, we also determine the time needed by the molecules to complete one round trip; these times are plotted as circles (○) in Fig. 3(b). In these measurements the velocity is held constant, and therefore the round trip time is also constant. We have also conducted measurements in which, starting after the 15^{th} round trip, we change the molecules' kinetic energy by 0.025 cm^{-1} per round trip. The arrival time of the accelerated and decelerated packets, indicated in Fig. 3(b), by up triangles (△) and down triangles (▽), respectively, are plotted as a function of round trip time.

Independent control over each half ring also enables the injection of multiple molecular packets into the ring without affecting the packet(s) that are already stored. Fig. 4 shows a similar measurement to that in Fig. 2, where we now inject a second packet 95.3 ms after injection of the first packet. In order to bunch both packets simultaneously, the fields are switched twice as often, i.e., we introduce a 'fake' gap at a quarter ring position. In this case, the second packet trails the first by 20 cm. In principle, we can load many more packets into the ring by introducing more 'fake' gaps. However, as molecules in a 'fake' gap experience a different transverse force as in a true gap, a more promising route is to construct a ring out of many short segments. As the symmetry of such a ring is higher, the transverse well will be deeper. Moreover, as the depth of the

longitudinal well is inversely proportional to the distance between the gaps, the longitudinal well will also be deeper.

Trapped molecules are being used for various precision tests and collision studies (an overview can be found in Bethlem and Meijer[18]). For many of these applications confining molecules in a ring rather than in a more conventional trap offers many advantages[10]. One of the most obvious applications is to use the ring as a neutral molecule collider. A stored packet of molecules revolving around the ring will meet counter-propagating packets. By storing many packets over an extended time, the sensitivity for detecting collisions increases by orders of magnitude. For instance, in a ring containing 10 packets revolving in both directions, a packet having completed 100 roundtrips will have had 2000 encounters. As the velocity of the beam is tunable, the collision cross-section can be measured as a function of beam energy, and resonances in the collision complex can be recorded – a low-energy molecular physics experiment as the ultimate replica of high-energy nuclear physics experiments.

Correspondence and requests for materials should be addressed to C.E.H. (e-mail: heiner@fhi-berlin.mpg.de) or H.L.B. (e-mail: rick@fhi-berlin.mpg.de).

Acknowledgements
We thank F.M.H. Crompvoets for help in the early stages of the project and for discussions. We acknowledge the technical assistance of A.J.A. van Roij and H. Haak and design and construction of the electronics by G. Heyne. This work was supported by the EU-network on "Cold Molecules". D.C. acknowledges support of the ESF Network on Collisions in Atom Traps (CATS). H.L.B acknowledges financial support from the Netherlands Organisation for Scientific Research (NWO) via a VENI-grant.

REFERENCES:

1) Paul, W. Electromagnetic traps for charged and neutral particles. *Rev. Mod. Phys.* **62**, 531-540 (1990).

2) Ido, T., and Katori, H. Recoil-free spectroscopy of neutral Sr in the Lamb-Dicke regime. *Phys. Rev. Lett.* **91**, 053001 (2003).

3) Cornell, E. A. & Wiemann, C. E. Bose-Einstein condensation in a dilute gas, the first 70 years and some recent results. *Rev. Mod. Phys.* **74**, 875-893 (2002).

4) Ketterle, W. When atoms behave as waves: Bose-Einstein condensation and the atom laser. *Rev. Mod. Phys.* **74**, 1131-1151 (2002).

5) Humphries Jr., S. *Principles of Charged Particle Acceleration.* (John Wiley and sons, Inc., New York, 1986).

6) Lee, S. Y. *Accelerator Physics* (second edition). (World Scientific, Singapore, 2004).

7) Kügler, K.-J., Paul, W. & Trinks, U. A magnetic storage ring for neutrons. *Phys. Lett. B* **72**, 422-424 (1978).

8) Sauer, J. A., Barrett, M. D. & Chapman, M. S. Storage ring for neutral atoms. *Phys. Rev. Lett.* **87**, 270401 (2001).

9) Crompvoets, F. M. H., Bethlem, H. L., Jongma, R. T. & Meijer, G. A prototype storage ring for neutral molecules. *Nature* **411**, 174-176 (2001).

10) Crompvoets, F. M. H., Bethlem, H. L. & Meijer, G. A storage ring for neutral molecules. *Adv. At. Mol. Opt. Phys.*, ed. P.R Berman and C. C. Lin, ISBN 0-12-003852-8, 52, 209-287 (2005).

11) Nishimura, H., Lambertson, G., Kalnins, J. G., and Gould, H. Feasibility of a synchrotron storage ring for neutral polar molecules. *Rev. Sci. Instrum.* **74**, 3271-3278, 2003.

12) Murch, K. W., Moore, K. L., Gupta, S. & Stamper-Kurn, D. M. Dispersion management using betatron resonances in an ultracold-atom storage ring. *Phys. Rev. Lett.* **96**, 013202 (2006).

13) Veksler, V. I. A new method for acceleration of relativistic particles, *Comptes Rendus de l'Academie des Sciences URSS* **43**, 329–331 (1944).

14) McMillan, E. M. The Synchrotron – a proposed high energy particle accelerator. *Phys. Rev.* **68**, 143-144 (1945).

15) Bethlem, H. L., Crompvoets, F. M. H., Jongma, R. T., van de Meerakker, S. Y. T. & Meijer, G. Deceleration and trapping of ammonia using time-varying electric fields. *Phys. Rev. A* **65**, 053416 (2002).

16) Gubbels, K., Meijer, G., and Friedrich, B. Analytic wave model of Stark deceleration dynamics. *Phys. Rev. A.* **73**, 063406 (2006).

17) Heiner, C. E., Bethlem, H. L. & Meijer, G. Molecular beams with a tunable velocity. *Phys. Chem. Chem. Phys.* **8**, 2666-2676 (2006).

18) Bethlem, HL & Meijer, G. Production and application of translationally cold molecules. *Int. Rev. Phys. Chem.* **22**, 73-128 (2003).

Fig. 1: Experimental set-up. ND_3 molecules with a velocity of 87 m/s (kinetic energy of 6.33 cm^{-1}) are tangentially injected into bend 1 of the segmented hexapole ring. The ring radius is 12.5 cm with two 2 mm gaps between the two halves; the diameter of the electrodes is 4mm. Molecules in the detection region are ionized using (2+1)-resonance enhanced multi-photon ionization (REMPI) with pulsed laser light around 317 nm, and are then extracted perpendicularly to the plane of the ring and counted by an ion detector. The four voltage configurations necessary for **(a)** confinement, **(b)** performing stop band correction, **(c)** acceleration/deceleration and bunching, and **(d)** extracting laser-ionized molecules, are shown. The contours represent the absolute electric field in steps of 8 kV/cm for (a), (b), and (c), and of 0.2 kV/cm for (d). Below, a time sequence is shown for molecules completing one round trip (without detection), starting from the arrow.

Fig. 2: Round trip time of flight (TOF) profiles. The density of ammonia molecules at the detection zone inside the synchrotron is shown as a function of storage time up to the 40^{th} round trip, currently limited only by our electronics. A zoom-in of two TOF profiles is shown as insets, more clearly illustrating the absolute widths of these peaks. From Gaussian fits to these profiles, we determine for the15^{th} round trip a temporal width of 55μs, corresponding to a position spread of 4.8 mm, and for the 40^{th} round trip a temporal width of 35μs, corresponding to a position spread of 3.0 mm.

Fig.3: Analysis of individual round trips. **(a)** The position spread of the stored molecules in the detection zone, determined from the TOF profiles shown in Fig. 2, is plotted as a function of the number of completed round trips, n. The inset shows the expansion of the molecules when they are released after the 4^{th} (△) and 25^{th} (□) round trip, respectively. The solid lines in the inset show the results from a simple fit $\Delta z(t) = (\Delta z_0^2 + (\Delta v_z \quad (t-t_0))^2)^{1/2}$, where Δz is the position spread, Δv_z is the velocity spread, t_0 is the time at which the packet has its minimum position spread (at the ¼ ring position), and Δz_0 is the position spread at that time.

(b) The round trip time, defined as t(n) – t(n-1), where t is the time of arrival and n is the number of completed round trips, is plotted as a function of n. Measurements are shown when the mean velocity of the packet is held constant (○), accelerated (△), or decelerated (▽).

Fig. 4: Multiple packets in the ring. TOF profiles showing two packets of ammonia molecules revolving inside the synchrotron. The second packet is injected 95.3 ms after the first packet, and trails it by 20 cm. Prior to injection of the second packet, the detection system is briefly switched off (indicated by the gray bar) to avoid saturation of the detector as the undecelerated part of the ammonia beam passes through the detection region. The alternating intensities observed arise from a less than ideal loading of the packet into the ring. The inset shows a zoom-in of a TOF profile of the first packet after completing its 11^{th} round trip and the second packet after completing its 1^{st} round trip.

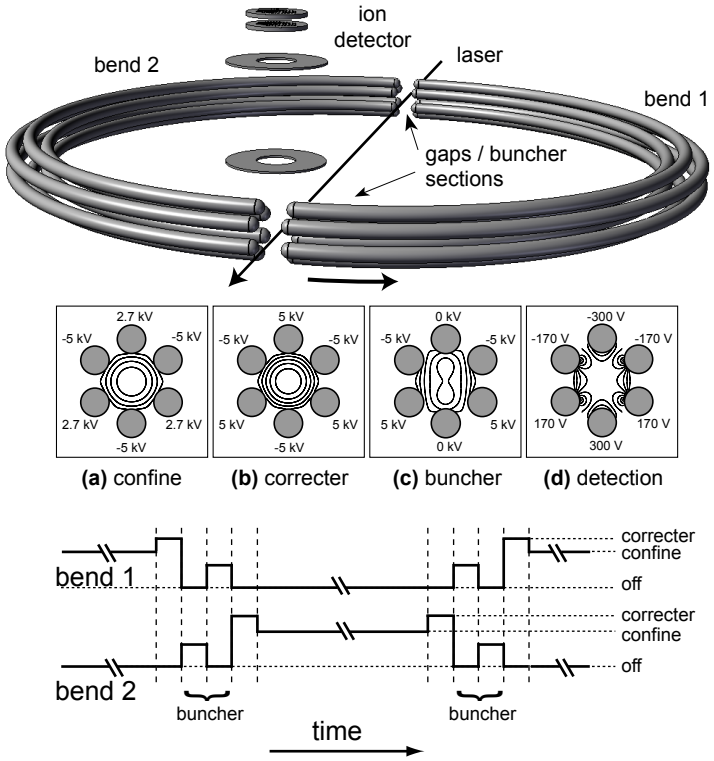

Figure 1, "A molecular synchrotron," Heiner et al.

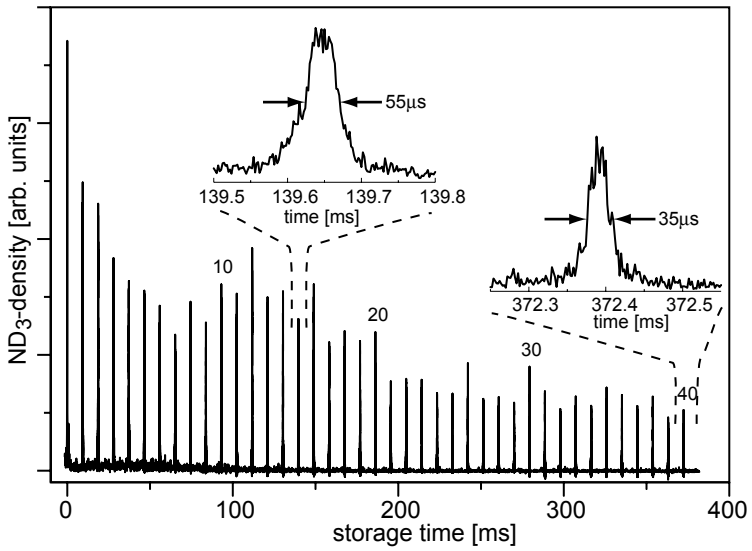

Figure 2, "A molecular synchrotron," Heiner et al.

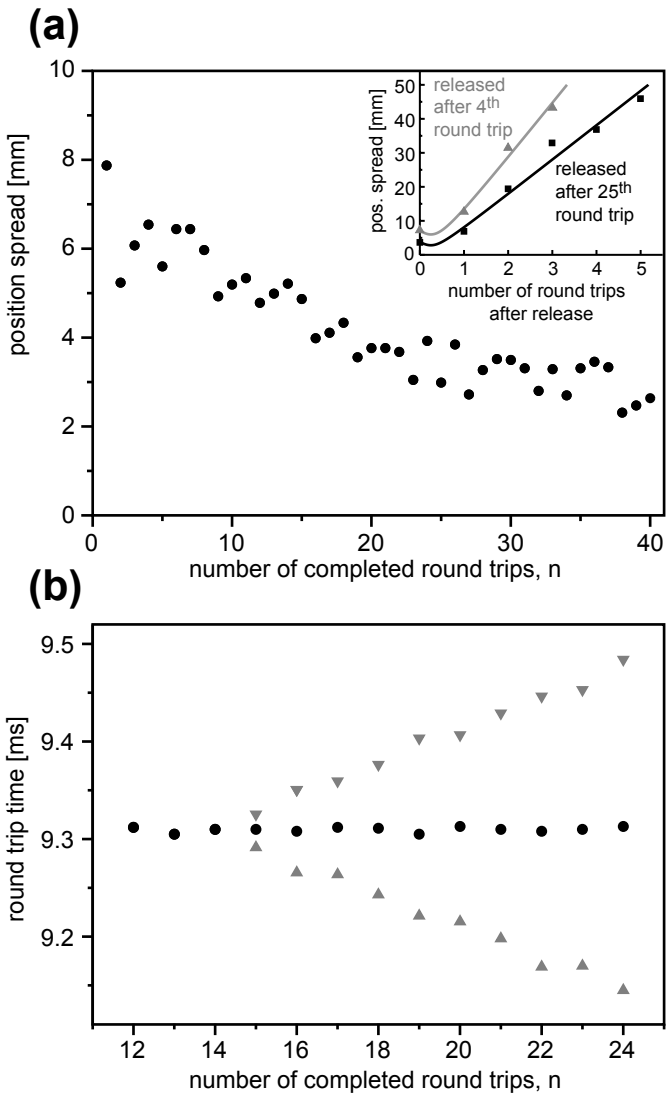

Figure 3, "A molecular synchrotron," Heiner et al.

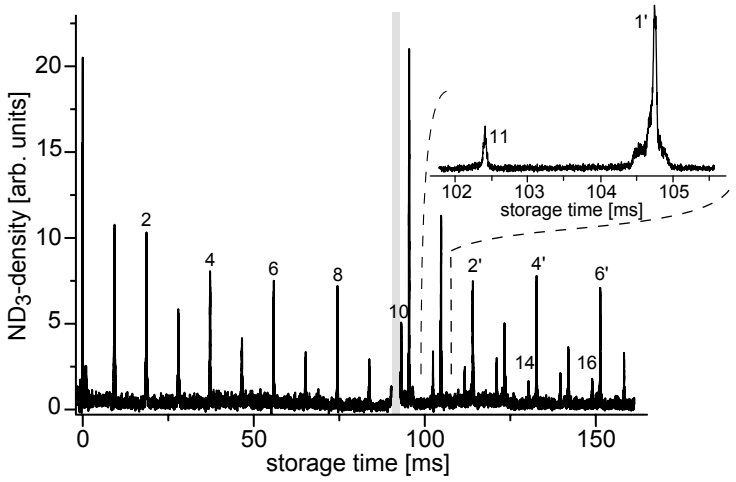

Figure 4, "A molecular synchrotron," Heiner et al.